IEEE Access
Multidisciplinary | Rapid Review | Open Access Journal

Received September 16, 2019, accepted October 7, 2019, date of publication October 24, 2019, date of current version November 6, 2019.

Digital Object Identifier 10.1109/ACCESS.2019.2949357

SOC Oriented Electrochemical-Thermal Coupled Modeling for Lithium-Ion Battery

YAN MA[1,2], XIN LI[2], GUANGYUAN LI[3], YUNFENG HU[1,2], AND QINGWEN BAI[4]

[1]State Key Laboratory of Automotive Simulation and Control, Jilin University, Changchun 130025, China
[2]Department of Control Science and Engineering, College of Communication Engineering, Jilin University, Changchun 130025, China
[3]School of Transportation Science and Engineering, Beihang University, Beijing 100000, China
[4]FAW-Volkswagen Automotive Company Ltd., Changchun 130025, China

Corresponding author: Yunfeng Hu (huyf@jlu.edu.cn)

ABSTRACT This paper proposes an electrochemical-thermal coupling model for state of charge (SOC) estimation of lithium-ion batteries (LIBs). In this paper, to solve two numerical problems in the quasi two-dimensional model of LIBs, a simplified one-dimensional model is built. Considering that the parameters in the model are affected by temperature, the internal parameters of the battery which obey the Arrhenius equation are introduced. Based on the simplified one-dimensional model, the electrochemical-thermal coupling model is built. Finally, an adaptive SOC observer based on electrochemical-thermal coupling model is designed. The simulation results show that the electrochemical-thermal coupling model can be effectively applied to SOC estimation.

INDEX TERMS Lithium-ion battery, pseudo two-dimensional, one-dimensional model, electrochemical-thermal coupling model, SOC estimation.

I. INTRODUCTION

Lithium-ion batteries (LIBs) are widely used in the field of electric vehicle power batteries due to their excellent performance [1]. In the battery management system (BMS), in order to optimize the overall performance of the system, it is necessary to build a lithium-ion battery model with high accuracy and low computational burden. Simultaneously, under the condition of high charge-discharge ratio, it is necessary to consider the temperature factor of the battery and build an electrochemical-thermal coupling model in order to describe the working mechanism of the battery more accurately [2]. In addition, it's important to estimate the state of charge (SOC) accurately for battery monitoring and usage, as the battery is a complex, closed system [3]. Therefore, model building and state estimation of LIBs also play a key role in BMS of electric vehicles [4].

The basic electrochemical model of lithium-ion batteries is a pseudo two-dimensional model which was built by Doyle [5]. This model can describe the working characteristics of LIBs during charging and discharging comprehensively and systematically. In application, the pseudo two-dimensional electrochemical model is faced with two main numerical problems [6]: (1) there are more states because of the existence of two dimensions; (2) The amount of calculation is large due to the existence of a large number of differential algebraic equations in the model. Common simplified models are electrochemical average model built by Domenico Di Domenico [7] and single particle model built by Santhanagopalan [8]. However, the electrochemical average model does not have a mature solution to the numerical problem (1), and the single particle model is not suitable for high charge-discharge ratio. Based on the previous research results, a new solution to the main numerical problems of pseudo two-dimensional model is proposed, which is to build a simplified one-dimensional model of LIBs by using dimensionality reduction and Padé approximation.

Usually, electrochemical-thermal coupling models are built for the following purposes: (1) improve the accuracy of the models; (2) study the safety performance of the battery; (3) used in the battery thermal management system; (4) SOC estimation [9]. In recent years, many new achievements have been made in the construction of electrochemical-thermal coupling models. However, the application of the simplified electrochemical-thermal coupling model is still relatively rare. Especially, the electrochemical-thermal coupling model for SOC estimation still has a large research space. In this paper, a new electrochemical-thermal coupling model

The associate editor coordinating the review of this manuscript and approving it for publication was Xinyu Du.

is established by coupling the simplified one-dimensional model with the concentrated mass thermal model and considering the Arrhenius equation of temperature dependence.

The model-based battery SOC estimation method represented by Kalman filter method is suitable for real-time application in BMS of electric vehicles [10]. At a larger charge-discharge ratio, temperature has a greater impact on battery performance, therefore battery temperature is an important parameter for SOC estimation. Some existing studies consider combining temperature parameters with equivalent circuit models to estimate the temperature of battery packs. Debert.M [11] built linear and time-varying observers to estimate the temperature of battery packs. However, due to the complexity of the model, the combination of electrochemical model and temperature model has been less studied.

In this paper, a new solution is proposed aiming at the main numerical problems of pseudo two-dimensional electrochemical model, that is, a simplified one-dimensional model of LIBs is built by using dimensionality reduction and Padé approximation. Based on the simplified one-dimensional model, a new electrochemical-thermal coupling model with the concentrated mass thermal model of the battery is established, and considering the Arrhhenius equation with temperature dependence of the battery parameters. On this basis, an adaptive SOC observer is established to analyze the asymptotic convergence of each estimator by Lyapunov, and the SOC of battery is estimated.

II. MODELING FOR LIBs

In this section, we develop the pseudo two-dimensional model and the simplified one-dimensional model of LIBs. Then the electrochemical-thermal coupling model based on simplified one-dimensional model is obtained for SOC estimation.

A. PSEUDO TWO-DIMENSIONAL MODEL OF LIBs

The structure of the pseudo two-dimensional model of LIBs based on physical and electrochemical principles is shown in Fig. 1. The pseudo two-dimensional model can be described as 6 equations: lithium-ion diffusion equation of electrolyte phase; lithium-ion diffusion equation of solid phase; electrolyte phase Ohm's law; solid phase Ohm's law; current balance equation; Butler-Volmer kinetics equation.

In order to explain the embedding and deembedding behavior of lithium-ions between solid phase and electrolyte phase, it is assumed that there exists a single dimensional solid spherical particle. Then the diffusion of lithium-ion in the particle can be described by Fick's second law in the spherical region.

$$\frac{\partial c_s}{\partial t} = \frac{1}{r^2}\frac{\partial}{\partial r}(D_s r^2 \frac{\partial c_s}{\partial r}) \tag{1}$$

where c_s is the concentration of lithium-ion of solid phase, D_s is the diffusion coefficient of solid phase, ∂r and ∂t represent the changes of c_s in the spatial and temporal scales of the radial direction of the sphere, respectively. The efficiency of

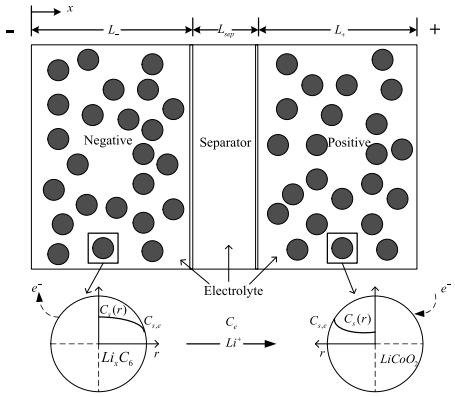

FIGURE 1. Structure of P2D model.

lithium-ion entering and leaving the solid phase is equal to the lithium-ion flux j_r at the solid phase-electrolyte phase interface on the particle surface and 0 at the particle center. The boundary condition of equation (1) is

$$\begin{cases} D_s \dfrac{\partial c_s}{\partial r}\Big|_{r=0} = 0 \\ D_s \dfrac{\partial c_s}{\partial r}\Big|_{r=R_s} = -\dfrac{j_r}{a_s}F \end{cases} \tag{2}$$

where $j_r > 0$ represents discharge, $j_r < 0$ represents charge, R_s is particle radius, a_s is the effective reaction area per unit volume of positive and negative electrodes, and F is Faraday constant.

For the lithium-ion diffusion of electrolyte phase, the equation is described as

$$\epsilon_e \frac{\partial c_e}{\partial t} = \frac{\partial}{\partial x}(D_e^{eff}\frac{\partial c_e}{\partial x}) + \frac{1-t_+^0}{F}j_r \tag{3}$$

where c_e is the lithium-ion concentration of electrolyte phase, D_e^{eff} is the effective diffusion coefficient of electrolyte phase, ϵ_e is the volume fraction of electrolyte phase, ∂x and ∂t represent the spatial and temporal scales of c_e along the x-axis in Cartesian coordinates, respectively. t_+^0 is lithium-ion transfer number of electrolyte phase. At the collector, the lithium-ion flow rate is zero, while at the junction of the positive and negative electrodes with the separator, the lithium-ion flow rate should be consistent, so the boundary conditions are obtained

$$\frac{\partial c_e^n}{\partial x}\Big|_{x=0} = \frac{\partial c_e^p}{\partial x}\Big|_{x=L_n+L_s+L_p} = 0 \tag{4}$$

where L_n, L_s, L_p are the thickness of negative, separator and positive respectively.

The equation of charge conservation in solid phase is

$$\sigma^{eff}\frac{\partial^2 \varphi_s}{\partial x^2} = j_r \tag{5}$$

where φ_s is solid potential and σ^{eff} is effective conductivity of solid phase. The electric field is proportional to the battery current at the collector and 0 at the separator. Therefore,

the boundary condition is

$$\begin{cases} -\sigma_n^{eff}\left.\dfrac{\partial\varphi_s^n}{\partial x}\right|_{x=0} = \sigma_p^{eff}\left.\dfrac{\partial\varphi_s^p}{\partial x}\right|_{x=L} = \dfrac{I}{A} \\ \left.\dfrac{\partial\varphi_s^n}{\partial x}\right|_{x=L_n} = \left.\dfrac{\partial\varphi_s^p}{\partial x}\right|_{x=L_n+L_s} = 0 \end{cases} \tag{6}$$

where $I > 0$ represents discharge, $I < 0$ represents charging, A represents positive and negative electrode area, $L = L_n + L_s + L_p$ represents battery thickness.

The equation of charge conservation in electrolyte phase is

$$\kappa^{eff}\frac{\partial^2\varphi_e}{\partial x^2} + \frac{\kappa_d^{eff}}{c_e, 0}\frac{\partial^2 c_e}{\partial x^2} + j_r = 0 \tag{7}$$

where φ_e is electrolyte potential; $\kappa_d^{eff} = \frac{2RT\kappa^{eff}}{F}(t_+^0 - 1)(1 + \frac{dlnf_\pm}{dlnc_e})$ is effective diffusion conductivity of electrolyte phase, $f_\pm$ is average molar activity coefficient of electrolyte phase, κ^eff is effective conductivity of electrolyte phase; R is Molar gas constant; T is cell temperature; d is differential sign. The boundary condition is

$$\left.\frac{\partial\varphi_e^n}{\partial x}\right|_{x=0} = \left.\frac{\partial\varphi_e^p}{\partial x}\right|_{x=L_n+L_s+L_p} = 0 \tag{8}$$

The Butler-Volmer equation describing the electrochemical reaction at the solid phrase-electrolyte phase interface is

$$j_r = a_s i_0[\exp(\frac{\alpha_a F\eta}{RT}) - \exp(\frac{\alpha_c F\eta}{RT})] \tag{9}$$

where

$$i_0(x,t) = kc_e^{\alpha_a}(c_{s,max} - c_{s,e})^{\alpha_a} c_{s,e}^{\alpha_c} \tag{10}$$

the over potential is

$$\eta = \varphi_s - \varphi_e - U \tag{11}$$

a_s is the active surface area per unit volume of the electrode; α_a, α_c are the transfer coefficient; $c_{s,e}$ is the lithium-ion concentration at the solid-electrolyte interface; $c_{s,max}$ is the maximum lithium-ion concentration of solid phase; U is open-circuit voltage.

In application, the pseudo two-dimensional electrochemical model faces two main numerical problems. One of the problems is the existence of a large number of state variables. As is shown in Fig. 1, the model has two dimensions: along the x-axis and along the solid spherical radial r-axis, the finite difference along the x-axis generates M states, while the finite difference along the radial r-axis generates N states. When the finite difference of the model along the x-axis is applied, the number of states falling on the diaphragm is about $\frac{1}{3}M$, which is not considered. Therefore the total number of states are about $\frac{2}{3}MN$. Secondly, the calculation of the model is complex. In about $\frac{2}{3}MN$ algebraic equations, most of them involve hyperbolic sinusoidal nonlinearity, resulting in a large number of differential-algebraic equations, which greatly increases the computational complexity.

Therefore, the simplification requirements of battery model are as follows: 1) reduce the dimensions of the model and state variables; 2) adopt appropriate numerical algorithms to deal with hyperbolic sinusoidal non-linear equations, so as to reduce the computational load.

B. SIMPLIFIED ONE-DIMENSIONAL MODEL OF LIBs

Firstly, aiming at the dimensionality problem of pseudo two-dimensional model, the one-dimensional model of battery is built based on the model in reference [12]. The hypothesis of one-dimensional model is: 1) the parameters are constant; 2) the lithium-ion flux j_r at the solid phase-electrolyte phase interface is decoupled from the lithium-ion concentration c_e in the electrolyte phase, and it is considered that c_e is constant. In one-dimensional model, the spatial variation of concentration is expressed as Warburg admittance form without dimension [13] by Laplace transformation of solid diffusion equation, and then the pseudo two-dimensional model is solved. c_s, c_e, η, φ_s, φ_e are unified as corresponding transfer function form.

Laplace transformation is applied to all the lithium-ion diffusion equations and charge conservation equations, and the model is transformed into a transfer function of finite order, which is more suitable for control engineering applications. Moreover, after the model is transformed from time domain to s domain, it does not need to be discretized from space, which greatly reduces the computational complexity of the model.

Firstly, r is regarded as a parameter, and the Laplace transformation of solid phase diffusion equation (1) can be obtained in spherical domain. Transform the equation (1) from the time domain to the s domain, then we can get the form of transfer function

$$\frac{d^2c_s(s)}{dr^2} + \frac{2}{r}\frac{dc_s(s)}{dr} - \frac{s}{D_s}c_s = 0 \tag{12}$$

In order to simplify, independent variables in $c_s(s)$ are omitted. Let $v = rc_s$, the equation (12) can be converted into

$$\frac{d^2v}{dr^2} - \frac{s}{D_s}v = 0 \tag{13}$$

In order to solve the equation conveniently, the function $\psi(r) = r\sqrt{s/D}$ is introduced, and the general solution of the equation (13) can be obtained as follow

$$c_s = \frac{A_0}{r}\exp[\psi(r)] + \frac{B_0}{r}\exp[-\psi(r)] \tag{14}$$

where A_0 and B_0 are undetermined coefficients. Let the diffusion start at r_0, the diffusion boundary at r_δ. The boundary condition is

$$\begin{cases} \dfrac{A_0}{r_\delta}E_\delta + \dfrac{B_0}{r_\delta}E_\delta^{-1} = 0 \\ D_s\left.\dfrac{dc_s}{dr}\right|_{r=r_0} = \dfrac{D_s}{r_0^2}(A_0(\psi(r_0) - 1)E_0 - B_0(\psi(r_0) + 1)E_0^{-1} \end{cases} \tag{15}$$

where $E_\delta = \exp[\psi(r_\delta)]$,$E_0 = \exp[\psi(r_0)]$.

From the general solution (14) and the boundary condition (15), we get

$$\frac{c_{s,e}(s)}{J_r(s)} = \frac{1}{a_s F}\frac{r_0}{D_s}[1+\frac{r_0}{r_\delta - r_0}\frac{\psi(r_\delta)-\psi(r_0)}{\tanh(\psi(r_\delta)-\psi(r_0))}]^{-1} \quad (16)$$

where $c_{s,e}(s)$ is the lithium-ion concentration at the solid phase-electrolyte phase interface. $J_r(s)$ is the lithium-ion flux density at the solid-liquid interface. In the diffusion of electrodes, it is considered that the diffusion is from the boundary to the center, so $r_\delta = 0$, $r_0 = R_s$. Equation (16) can be reduced to

$$\frac{c_{s,e}(s)}{J_r(s)} = \frac{1}{a_s F}\frac{R_s}{D_s}[\frac{\tanh(R_s\sqrt{s/D_s})}{\tanh(R_s\sqrt{s/D_s}) - R_s\sqrt{s/D_s}}] \quad (17)$$

Equation (17) is the transfer function of solid phase diffusion. Thus, the problem of two dimensions in the pseudo two-dimensional model is solved. The one-dimensional model can be obtained by Laplace transformation and solution of electrolyte phase lithium-ion diffusion, solid phase potential, electrolyte phase potential and Butler-Volmer equation. Then the Butler-Volmer dynamic equation is linearized.

$$\eta = \frac{R_{ct}}{a_s}J_r \quad (18)$$

where $R_{ct} = RT/[i_0\, F(\alpha_a + \alpha_c)]$.

For the solid charge conservation equation (5), the integrals are obtained in two electrode regions and the boundary conditions (6) are substituted. For Laplace transformation, we get

$$\begin{cases} \dfrac{J_{r,p}(s)}{I(s)} = -\dfrac{I}{AL_p} \\ \dfrac{J_{r,n}(s)}{I(s)} = -\dfrac{I}{AL_n} \end{cases} \quad (19)$$

where I is the input current. In the electrolyte phase, since the distribution of J_r in the positive and negative electrodes can offset the change of lithium-ion concentration in the electrolyte phase, c_e is taken as a fixed value. Then the normalized current density is substituted into the charge conservation equation of electrolyte phase (7). Negative pole, positive pole and separator are considered respectively, and then Laplace transformation is carried out.

$$\kappa_n^{eff}\frac{\partial^2\varphi_e^n(s)}{\partial x^2} + \frac{a_{s,n}F}{AL_n}I(s) = 0, \quad x \in (0, L_n) \quad (20)$$

$$\kappa_s^{eff}\frac{\partial^2\varphi_e^s(s)}{\partial x^2} + I(s) = 0, \quad x \in (L_n, L_n + L_s) \quad (21)$$

$$\kappa_p^{eff}\frac{\partial^2\varphi_e^p(s)}{\partial x^2} - \frac{a_{s,n}F}{AL_n}I(s) = 0, \quad x \in (L_n + L_s, L) \quad (22)$$

where φ_e^n, φ_e^s, φ_e^p are the potential of positive, separator and negative electrodes, and κ_n^{eff}, κ_s^{eff}, κ_p^{eff} are the effective conductivity of positive, separator and negative electrodes, which is assumed to be constant in all domains. $a_{s,n}$, $a_{s,p}$ are the active surface area per unit volume of positive and negative electrodes. Definite the potential difference of electrolyte phase

$$\Delta\varphi_e^n(x, s) = \varphi_e^n(x, s) - \varphi_e^n(0, s), \; x \in (0, L_n) \quad (23)$$

$$\Delta\varphi_e^s(x, s) = \varphi_e^s(x, s) - \varphi_e^n(0, s), \; x \in (L_n, L_n + L_s) \quad (24)$$

$$\Delta\varphi_e^p(x, s) = \varphi_e^p(x, s) - \varphi_e^n(0, s), \; x \in (L_n + L_s, L) \quad (25)$$

consider $\varphi_e^n(0, s)$ as zero potential, we can get

$$\Delta\varphi_e^n(x, s) = -\frac{a_{s,n}F}{6\kappa_n^{eff}AL_n}I(s)x^3 \quad (26)$$

$$\Delta\varphi_e^s(x, s) = -\frac{1}{2\kappa_n^{eff}}I(s)(x - x_n)^2 \quad (27)$$

$$\Delta\varphi_e^p(x, s) = -\frac{a_{s,p}F}{6\kappa_n^{eff}AL_p}I(s)(x - x_p)^3 \quad (28)$$

After simplification,

$$\frac{\Delta\varphi_e(L, s)}{I(s)} = -\frac{a_{s,p}FL_n^2}{6\kappa_n^{eff}A} - \frac{L_s^2}{2\kappa_n^{eff}} - \frac{a_{s,p}FL_n^2}{6\kappa_p^{eff}A} \quad (29)$$

The battery terminal voltage is expressed as

$$V(t) = \varphi_s(L, t) - \varphi_s(0, t) - \frac{R_f}{A}I(t) \quad (30)$$

where the R_f is the membrane resistance of the battery. The expression of overpotential (11) is substituted for the expression of terminal voltage (30), and the expression of terminal voltage (30) can be extended to

$$V(t) = \varphi_e(L, t) - \varphi_e(0, t) + \eta(L, t) - \eta(0, t) + U_+(c_{s,e}(L, t)) - U_-(c_s, e(0, t)) - \frac{R_f}{A}I(t) \quad (31)$$

After Laplace transform, the voltage expression is

$$\frac{V(s)}{I(s)} = \frac{\Delta\varphi_e(L, s)}{I(s)} + \frac{\eta_p(L, s)}{I(s)} - \frac{\eta_n(0, s)}{I(s)} + \frac{\partial U_p}{\partial c_{s,e}}\frac{c_{s,e}^p(L, s)}{I(s)} - \frac{\partial U_n}{\partial c_{s,e}}\frac{c_{s,e}^n(L, s)}{I(s)} - \frac{R_f}{A} \quad (32)$$

where $\frac{\partial U_p}{\partial c_{s,e}}$ $\frac{\partial U_p}{\partial c_{s,e}}$ are the slope of the open-circuit voltage, which can be calibrated at different SOC by means of experimental measurement.

The one-dimensional model proposed by the author solves the problem of dimensionality of pseudo two-dimensional model through reasonable transformation and simplification, and reduces the computational load of the model to a certain extent. However, the solid-phase diffusion equation in one-dimensional model is still transcendental equation with complex calculation, so numerical method is needed to simplify the order reduction. The characteristics of diffusion equation are: 1) countable infinite poles; 2) spherical diffusion. Considering these two characteristics, Padé approximation is used to simplify the algorithm. Padé approximation is a rational polynomial approximation method, which can effectively approximate spherical problems at low frequencies and avoid spatial dispersion. The problem of infinite poles can be approximated by analytic method.

Firstly, by introducing $s = Ds^*/R$ and omitting the coefficients, the transcendental transfer function (17) is transformed to obtain

$$G(s) = \frac{\sinh(\sqrt{s^*})}{\sinh(\sqrt{s^*}) - \sqrt{s^*}\cosh(\sqrt{s^*})} \quad (33)$$

According to Padé approximation principle, equation (33) needs to be extended to power series passing through the origin. Firstly, the two sides of equation (33) are multiplied by s^*, and then the $s^*G(s)$ is expanded by power series at the origin.

$$s^*G(s) = -3 - \frac{1}{5}s^* + \frac{1}{175}s^{*2} - \frac{2}{7875}s^{*3} + \frac{37}{3031875}s^{*4} + \cdots \quad (34)$$

The Padé approximate transfer function is

$$sP(s) = \sum_{m=0}^{M} b_m s^m / (1 + \sum_{n=1}^{N} a_n s^n) \quad (35)$$

where the order of molecules and denominators can be selected, and the order of molecules is less than or equal to the order of denominators in Padé approximation. In order to balance the accuracy and computational complexity, the third-order Padé approximation is used to simplify the algorithm. There is

$$sP(s) = \frac{b_0 + b_1 s + b_2 s^2}{1 + a_1 s + a_2 s^2} \quad (36)$$

Thus, the linear equations for solving the coefficients in $P(s)$ are determined by the following polynomials

$$\begin{aligned} &\frac{37a_2}{3031875}s^6 + (\frac{37a_1}{3031875} - \frac{2a_2}{7875})s^5 + (\frac{37}{3031875} \\ &-\frac{2a_1}{7875} + \frac{a_2}{175})s^4 + (-\frac{2}{7875} + \frac{a_1}{175} - \frac{a_2}{5})s^3 \\ &+(\frac{1}{175} - \frac{a_1}{5} - 3a_2 - b_2)s^2 + (-\frac{1}{5} - 3a_1 - b_1)s \\ &-3 - b_0 = 0 \end{aligned} \quad (37)$$

For all s equations, the right side is zero, so the coefficient must be zero. Two equations of unknown numbers a_1 and a_2 are obtained from s^4 and s^3. Then, the equations of b_0, b_1 and b_2 are obtained from s^2, s and constant terms. By substituting these solutions into equation (36), we get

$$G(s^*) \approx P(s^*) = \frac{-3 - \frac{4}{11}s^* - \frac{1}{165}s^{*2}}{s^* + \frac{3}{55}s^{*2} + \frac{1}{3465}s^{*3}} \quad (38)$$

The normalized current density, coefficient and $S = Ds^*/R$ are substituted into the equation (38), and the solid phase diffusion transfer functions of positive and negative electrodes are obtained respectively.

$$\frac{C^n_{s,e}(s)}{I(s)} = \frac{21[\frac{1}{\Xi_n R^n_s}s^2 + \frac{60D^n_s}{\Xi_n (R^n_s)^3}s + \frac{495(D^n_s)^2}{\Xi_n (R^n_s)^5}]}{s^3 + \frac{189D^n_s}{(R^n_s)^2}s^2 + \frac{3465(D^n_s)^2}{(R^n_s)^4}s} \quad (39)$$

$$\frac{C^p_{s,e}(s)}{I(s)} = \frac{21[\frac{1}{\Xi_p R^p_s}s^2 + \frac{60D^p_s}{\Xi_p (R^p_s)^3}s + \frac{495(D^p_s)^2}{\Xi_p (R^p_s)^5}]}{s^3 + \frac{189D^p_s}{(R^p_s)^2}s^2 + \frac{3465(D^p_s)^2}{(R^p_s)^4}s} \quad (40)$$

where $\Xi_n = a^n_s FAL_n, \Xi_p = a^p_s FAL_p$.

Before using the model for SOC estimation, it is necessary to preliminarily verify the accuracy of the model, and verify

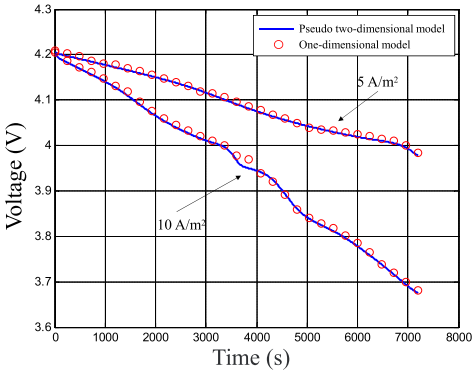

(a) $5A/m^2$, $10A/m^2$

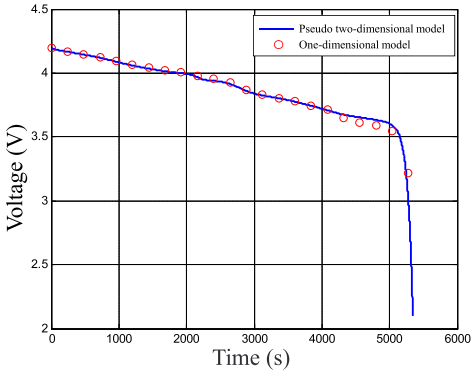

(b) $15A/m^2$

FIGURE 2. Comparison of voltages at different discharging current densities ($5A/m^2$, $10A/m^2$ and $15A/m^2$). (a) $5A/m^2$, $10A/m^2$. (b) $15A/m^2$.

that the simplified processing of one-dimensional model is reasonable and effective. The paper compares the proposed one-dimensional model with the pseudo two-dimensional model of the exact model, that is, the pseudo two-dimensional model is taken as the exact value. In order to verify the validity of the proposed model, the charging and discharging experiments of LIBs with positive $LiCoO_2$ and negative MCMB2528 are carried out under different operating conditions, and the current and voltage data are obtained. The battery model is NCR18650B, with a diameter of 18 mm and a length of 65 mm. The geometric characteristics are shown in the figure. The battery capacity is 3400 mAh, rated voltage is 3.7V, with the upper voltage of 4.2V.

The mathematical model of LIBs in this subject is very complex, and the mathematical function can not express the relationship between output and input. The genetic algorithm has no requirement for the equation of the simulation model and neglects the complex influence of the battery model. Therefore, the genetic algorithm is used to identify the main parameters of the model. The other parameter values are shown in Table 1.

The electrochemical charging and discharging characteristics of LIBs are simulated by using MATLAB/Simulink and Fortran programs. Fig 2-5 are simulation results. Fig 2 shows the comparison of model terminal voltage under different discharge current densities ($5A/m^2$, $10A/m^2$, $15A/m^2$). Fig

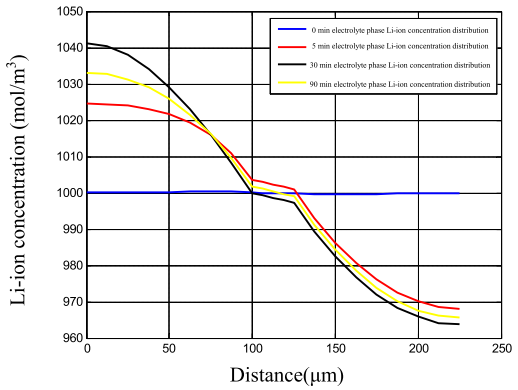

FIGURE 3. Electrolyte Li-ion concentration at different time points for $15A/m^2$ discharging.

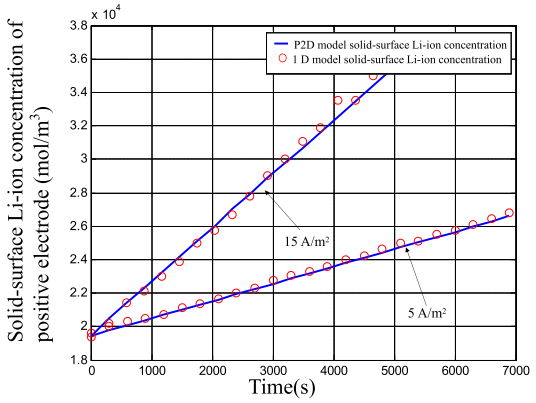

(a) positive electrode

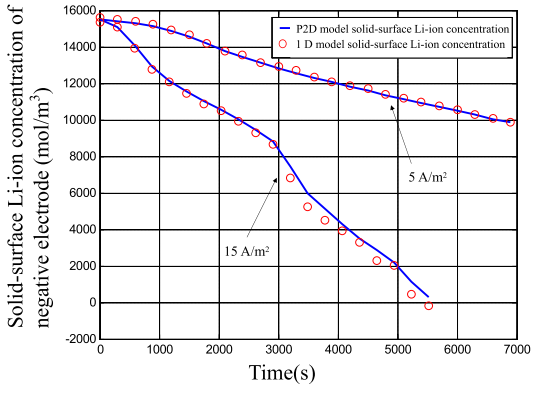

(b) negative electrode

FIGURE 4. Comparison of lithium-ion concentration on solid surface at different discharge current densities ($5A/m^2$,$15A/m^2$).

3 shows the distribution of lithium-ion concentration in electrolyte phase at different discharge time (starting time, 5 min, 30 min, 90 min). Fig 4 and Fig 5 are comparisons of lithium-ion concentration on solid surface of positive and negative electrodes at different discharge current densities ($5A/m^2$, $15A/m^2$). The current density of $10\,A/m^2$ is omitted, and only the discharge with lower current density and higher current

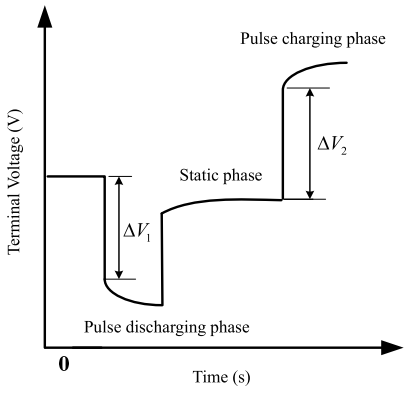

FIGURE 5. Measurement method of battery internal resistance pulse charging and discharging.

density is considered to verify whether the Padé approximation has better calculation effect at higher discharge rate.

As can be seen from Fig 2, with the increase of discharge current density, the error of the model increases, but the overall accuracy remains high.

For the lithium-ion diffusion of electrolyte phase, it can be seen from Fig 3 that it is reasonable to choose a constant electrolyte phase concentration of 1000 mol/m^3 as the initial concentration. As shown in Fig 4 and Fig 5, the model can maintain high accuracy. It proves the accuracy and validity of simplifying the solid phase diffusion equation by using Padé approximation method.

C. ELECTROCHEMICAL-THERMAL COUPLING MODEL BASED ON SIMPLIFIED ONE-DIMENSIONAL MODEL

Some parameters in the battery electrochemical model are greatly affected by temperature, such as contact resistance R_f, electrochemical reaction rate k, solid diffusion coefficient D_s and so on. The change of temperature has a great influence on the accuracy of the model. In this section, the thermal characteristics of LIBs are studied firstly, and then a lumped mass thermal model is built based on Bernadi equation. Finally, an electrochemical-thermal coupling model of LIBs is built according to Arrhenius equation.

The internal heat generation of the battery is mainly composed of four parts: the heat Q_r generated by electrochemical reaction, the heat Q_p generated by polarization of the electrode, the heat Q_j generated by internal resistance through current and the heat Q_s generated by decomposition of substances in the battery.

The decomposition of electrolyte produces flammable gas when charging is completed. The heat of decomposition is the heat generated by the irreversible reaction. In general, functions are designed to prevent this phenomenon, so the heat of decomposition is usually neglected.

The total heat Q_t generation of lithium-ion phosphate batteries can be expressed as:

$$Q_t = Q_r + Q_p + Q_j = nFT(-\frac{\delta E_e}{\delta T}) + Q_p + Q_j \quad (41)$$

TABLE 1. MCMB/$LiCoO_2$ battery parameters.

Parameters	Negative	Positive	Diaphragm
Thickness L/cm	$50 * 10^{-4}$	$25.4 * 10^{-4}$	$36.4 * 10^{-4}$
Particle Radius R/cm	$1 * 10^{-4}$		$1 * 10^{-4}$
Volume Ratio of Active Materials ϵ_s	0.662		0.58
Porosity ϵ_e	0.3	0.4	0.3
Maximum Solid Concentration	$1.61 * 10^{-2}$		$2.39 * 10^{-2}$
0% SOC Stoichiometry $x_{0\%}, y_{0\%}$	0.001		0.955473
100% SOC Stoichiometry $x_{0\%}, y_{0\%}$	0.790813		0.359749
Average Electrolyte Concentration $c_{e,0}/(mol \cdot cm^{-3})$		$1.0 * 10^{-3}$	
Charge transfer Coefficient α_a α_c	0.5,0.5		0.5,0.5
Lithium-Ion Li^+ Migration Number t_0^+		0.38	
Membrane Resistance R_f/Ω		$20 * 10^{-3}$	
Diffusion Coefficient of Solid Lithium-ion $D_{s,ref}/(cm^2 \cdot s^{-1})$	$3.9447 * 10^{-10}$		$1.0156 * 10^{-9}$
Electrode Plate Area A/cm^2		1020.41	

The heat balance per unit time during charging can be expressed as:

$$\begin{aligned} Q_t &= Q_c = Q_r + Q_{pc} + Q_j \\ &= -3.73 \times 10^{-2} Q_1 I_c + 3.60 I_c^2 R_p c + 3.60 I_c^2 R_e c \\ &= -3.73 \times 10^{-2} Q_1 I_c + 3.60 I_c^2 R_t c (KJ/h) \end{aligned} \tag{42}$$

In the lumped mass thermal model, we neglect the spatial distribution of cell temperature. So temperature T is a function of time. The energy balance equation of the lumped mass heat model is as follows:

$$\begin{aligned} \rho v C_p \frac{dT}{dt} &= I(U_p(c_{s,e}^p, T) - U_n(C_{s,e}^n, T) - V) \\ &\quad - IT\left(\frac{\partial U_p}{\partial T} - \frac{\partial U_n}{\partial T}\right) - q \end{aligned} \tag{43}$$

where the initial temperature of the battery is assumed to be ambient temperature, that is $T|_{t=0} = T_\infty$; ρ is the density of the battery; v is the volume of the battery; C_p is the specific heat capacity of the battery; $U_p(c_{s,e}^p, T)$ and $U_n(c_{s,e}^n, T)$ are functions of $c_{s,e}^p$ and $c_{s,e}^n$; q is the heat exchange between the battery and the environment.

The heat exchange on the surface of batteries obeys Newton's cooling law. There are:

$$q = hA(T - T_\infty) \tag{44}$$

where h is the heat transfer coefficient; A is the surface area of the battery.

In the energy balance equation, the first term $I(U_p(c_{s,e}^p, T) - U_n(C_{s,e}^n, T) - V)$ on the right side is irreversible heat generation generated by the polarization of the electrode,which is always positive regardless of whether the charge or discharge. The second item $IT(\frac{\partial U_p(c_{s,e}^p, T)}{\partial T} - \frac{\partial U_n(c_{s,e}^n, T)}{\partial T})$ is the reversible heat production produced by the change of electrochemical reaction entropy. The value of reversible heat can be positive or negative, depending on the direction of the electrochemical reaction.

In the lumped mass thermal model, the heat change of the battery is determined by the reversible heat, irreversible heat and heat exchange with the environment.

Generally, the relationship between the solid phase diffusion coefficient D_s, the rate constant k of electrochemical reaction and temperature can be described by Arrhenius equation. In addition, there is a functional relationship between contact resistance R_f and temperature. For simplification, we assume that the relationship between contact resistance and temperature is linear. It can be expressed as:

TABLE 2. MCMB/$LiCoO_2$ battery parameters of temperature model.

Parameters	Negative	Positive	Diaphragm
activation energy of D_s	1.663	7.483	
activation energy of D_e			16.628
activation energy of $kappa$			13.756
activation energy of k	14.965	14.965	
activation energy of R_f	14.965	14.965	

$$k(T) = k_{ref} \exp\left(\frac{E_k}{R}\left(\frac{1}{T} - \frac{1}{T_\infty}\right)\right) \tag{45}$$

$$D_s(T) = D_{s,ref} \exp\left(\frac{E_{D_s}}{R}\left(\frac{1}{T} - \frac{1}{T_\infty}\right)\right) \tag{46}$$

$$R_f(T) = R_{f,0} + \alpha T \tag{47}$$

where $k(T)$ is divided into $k_p(T)$ and $k_n(T)$, representing the rate constant of electrochemical reaction of positive and negative electrodes, $D_s(T)$ is divided into $D_{s,p}(T)$ and $D_{s,n}(T)$, representing the solid diffusion coefficient of positive and negative electrodes, k_{ref} is divided into $k_{p,ref}$ and $k_{n,ref}$, representing the reference value of rate constant of electrochemical reaction of positive and negative electrodes at ambient temperature, $D_{s,ref}$ is divided into $D_{s,p,ref}$ and $D_{s,n,ref}$, representing the reference value of solid diffusion coefficient of positive and negative electrodes at ambient temperature, and $R_{f,0}$ is the constant part of contact resistance. α is the proportional coefficient.

In this paper, experimental identification and literature search are combined to obtain model parameters.

Through literature search, the activation energy parameters of temperature-dependent solid diffusion coefficient D_s and electrochemical reaction rate constant k in Table 2 are obtained, and the relations between open-circuit voltage and state of charge are given in equation (48)-(51). In addition, the parameters that need to be determined are the functional relationship between contact resistance and temperature.

The positive equilibrium potential function is

$$U_p(\theta_p) = 85.681\theta_p^6 - 357.70\theta_p^5 + 613.89\theta_p^4 - 555.65\theta_p^3 + 281.06\theta_p^2 - 76.648\theta_p + 13.1983 - 0.30987\exp(\theta_p^{115}) \quad (48)$$

The negative equilibrium potential function is

$$U_n(\theta_n) = 8.0029 - 5.0647\theta_n + 12.578\theta_n^{0.5} - 8.6332\times10^{-5}\theta_n^{-1} + 2.1765\times10^{-4}\theta_n^{1.5} - 0.46016\exp[15.0(0.06-\theta_n)] - 0.55364\exp[-2.4326(\theta_n-0.92)] \quad (49)$$

The temperature coefficient of the positive equilibrium potential is

$$\frac{\partial U_p}{\partial T} = \frac{-0.19952+0.92837\theta_p-1.36455\theta_p^2+0.61154\theta_p^3}{1-5.66148\theta_p+11.4763\theta_p^2-9.8243\theta_p^3+3.04876\theta_p^4} \quad (50)$$

The temperature coefficient of the negative equilibrium potential is

$$\frac{\partial U_p}{\partial T} = \frac{0.0052+3.2992\theta_n-91.7932\theta_n^2+1004.9110\theta_n^3}{1-48.0982\theta_n+1017.2348\theta_n^2-10481.8041\theta_n^3} \frac{-5812.2781\theta_n^4+19329.7549\theta_n^5-37147.8947\theta_n^6}{+59431.3000\theta_n^4+195881.6488\theta_n^5-374557.3152\theta_n^6} \frac{+38379.1812\theta_n^7-16515.0530\theta_n^8}{+385821.1607\theta_n^7-165705.8597\theta_n^8} \quad (51)$$

$LiCoO_2$ cathode and MCMB2528 cathode LIBs are also used as experimental subjects. It is considered that the value of contact resistance is the internal resistance of the battery. The schematic diagram for measuring the internal resistance of battery charging and discharging is shown in Fig 5. The discharge resistance R_D and charge resistance R_c of batteries are solved by equation (52) and equation (53).

$$R_D = \frac{\Delta V_1}{\Delta I} \quad (52)$$

$$R_D = \frac{\Delta V_2}{\Delta I} \quad (53)$$

In order to obtain the curve of internal resistance varying with temperature, 600 mA current is set to discharge experiment for reference model. The middle section is stopped every 5% or 10% SOC, and the voltage and current datas of battery are recorded. Through data processing and identification of ohmic internal resistance of batteries at different temperatures, the expression of internal resistance can be obtained as shown in equation (54). The curve of internal resistance changing with temperature is shown in Fig 6.

$$R_f(T) = R_{f,0} + \alpha T \quad (54)$$

where the parameters of target battery are $\alpha = -0.134$, $R_{f,0} = 19.67$.

In order to verify the accuracy of the electrochemical-thermal coupling model, the pseudo two-dimensional model considering temperature is used as the reference model to compare the accuracy of the electrochemical-thermal coupling model and the one-dimensional model. The experiments of LIBs (capacity of 3400 mAh,rated voltage of 3.7V) with positive $LiCoO_2$ and negative MCMB2528 are carried out and use MATLAB / Simulink and FORTRAN program to

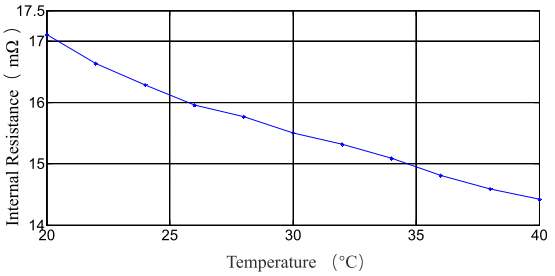

FIGURE 6. The internal resistance of lithium batteries varies with temperature.

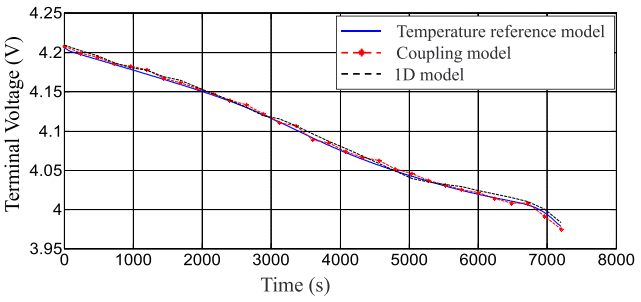

(a) $5A/m^2$

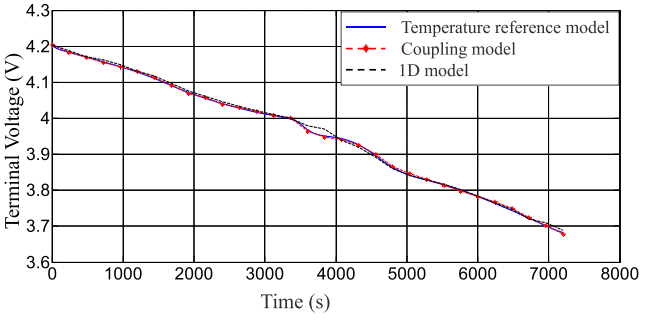

(b) $10A/m^2$

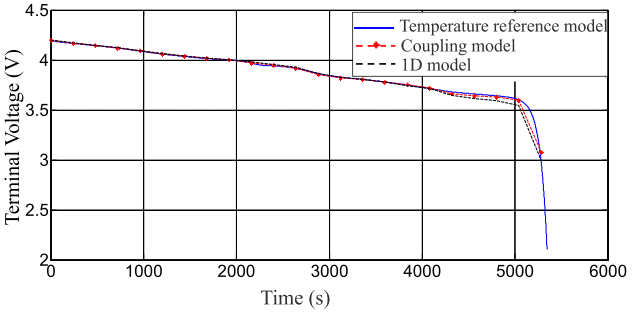

(c) $15A/m^2$

FIGURE 7. Comparison of terminal voltage at different discharge current densities ($5A/m^2$,$10A/m^2$,$15A/m^2$).

simulate. Fig 7 shows 30 sampling points under the different discharge current density ($5A/m^2$, $10A/m^2$, $15A/m^2$) respectively, and compares the terminal voltage of the built model and the reference model.

As can be seen in Fig 7, as the discharge current increases, the battery temperature increases. The error of electrochemical thermal coupling model is lower than that of one-dimensional model without considering temperature. The error is about 1.75%.

III. SOC ESTIMATION BASED ON ELECTROCHEMICAL-THERMAL COUPLING MODEL

Based on the electrochemical-thermal coupling model built in the previous section, SOC observer is designed.

A. SOC OBSERVER ARCHITECTURE

Firstly, the coupling model should be transformed into the form of state space equation. According to the equation (39) and equation (40), the state space equation of solid phase diffusion can be obtained as follows:

$$\begin{aligned} \dot{c_s} &= A_i c_s + B_i I \\ c_{s,e} &= C_i c_s \end{aligned} \tag{55}$$

where c_s lithium-ion concentration; $c_{s,e}$ is surface lithium-ion concentration; A_i,B_i,C_i are express as:

$$A_n = \begin{bmatrix} 0 & 1 & 0 \\ 0 & 0 & 1 \\ 0 & -\dfrac{3465(D_s^n)^2}{(R_s^n)^4} & -\dfrac{189D_s^n}{(R_s^n)^2} \end{bmatrix}$$

$$A_p = \begin{bmatrix} 0 & 1 & 0 \\ 0 & 0 & 1 \\ 0 & -\dfrac{3465(D_s^p)^2}{(R_s^p)^4} & -\dfrac{189D_s^p}{(R_s^p)^2} \end{bmatrix}$$

$$B_n = B_p = \begin{bmatrix} 0 & 0 & 1 \end{bmatrix}^T$$

$$C_n = \begin{bmatrix} -\dfrac{10395(D_s^n)^2}{a_s^n FA(R_s^n)^5 L_n} & -\dfrac{1260D_s^n}{a_s^n FA(R_s^n)^3 L_n} & -\dfrac{21}{a_s^n FAR_s^n L_n} \end{bmatrix}^T$$

$$C_p = \begin{bmatrix} -\dfrac{10395(D_s^p)^2}{a_s^n FA(R_s^p)^5 L_p} & -\dfrac{1260D_s^p}{a_s^n FA(R_s^p)^3 L_p} & -\dfrac{21}{a_s^p FAR_s^p L_p} \end{bmatrix}^T$$

Based on the [14], the thermal model equation (43) is approximated:

$$U_p(C_{s,e}^p, T) \approx U_p(C_{s,e}^p, T_\infty) + \frac{\partial U_p}{\partial T}(T - T_\infty) \tag{56}$$

$$U_n(C_{s,e}^n, T) \approx U_n(C_{s,e}^n, T_\infty) + \frac{\partial U_n}{\partial T}(T - T_\infty) \tag{57}$$

Substituting equation (43), we can get

$$\begin{aligned} \rho v C_p \frac{dT}{dt} &= I(U_p(C_{s,e}^n, T_\infty) + \frac{\partial U_p}{\partial T}(T - T_\infty) \\ &\quad - U_n(C_{s,e}^n, T_\infty) - \frac{\partial U_n}{\partial T}(T - T_\infty) - V) \\ &\quad - IT(\frac{\partial U_p(c_{s,e}^p, T)}{\partial T} - \frac{\partial U_n(c_{s,e}^n, T)}{\partial T}) - hA(T - T_\infty) \\ &= I(U_n(C_{s,e}^p, T_\infty) - \frac{\partial U_p}{\partial T}T_\infty - U_n(C_{s,e}^n, T_\infty) \\ &\quad + \frac{\partial U_n}{\partial T}T_\infty - V) - hA(T - T_\infty) \end{aligned} \tag{58}$$

In summary, the state space model of LIBs, including thermal model and electrochemical model, is expressed as a single input and double output system. Input u is current I, output y_1 is terminal voltage V, y_2 is temperature T. The state quantity x_1 is the lithium-ion concentration state c_s, and the state quantity x_2 is the temperature T. The state space equation is constructed as

$$\begin{aligned} \dot{x_1} &= \theta f_1(x_2) A x_1 + Bu \\ \dot{x_1} &= u f_2(x_{1,3}, x_2, y_1) - k_1(x_2 - x_{2,\infty}) \\ y_1 &= f_3(x_{1,3}, x_2, u) - R_{f,0}u - \alpha x_2 u \\ y_2 &= x_2 \end{aligned} \tag{59}$$

where $x_1 = [c_{s1}, c_{s2}, c_{s3}]^T$ is the state variables of the transfer function of the relationship between lithium-ion concentration and current on the solid surface after Padé approximation treatment. It has no practical physical significance except for the surface lithium ion concentration $c_{s,3}$. $x_{1,3} = x_1(3) = c_{s,3}$ is the surface concentration state; x_2 is the temperature state, $x_{2,\infty}$ is the room temperature; $\theta = D_{s,ref}^-/\Delta^2$ is the scalar parameter related to the diffusion coefficient; $R_{f,0}$ is the constant part of the contact resistance and α is the part of contact resistance changing with temperature, which is identified in the previous section; y_1 is the measuring voltage; y_2 is the measuring temperature; u is the measuring current; f_1 is the temperature function given by the exponential term in the Arrhenius equation; f_2 is the thermal part. The scalar function given by the model; $k \in R$ is a parameter of Newton's law of heat dissipation, that is, the thermal exchange coefficient multiplied by the surface area of the battery; f_3 is a scalar function obtained from the terminal voltage equation. Note that A is the matrix of state space equation transformed by the transfer function, which is not the same as the cell surface area A in the previous section.

The characteristics of the state space equation are as follows:

(1) Functions f_1, f_2 and f_3 are all constrained functions, and f_1 is positive.

(2) The local observability of the system can be proved by linearizing the system at different working points and using the rank condition of the observable matrix to prove it.

(3) Output y is a monotonic increasing function of surface concentration x at given current and temperature. Therefore, we can get: given any $u = u^*$, $x_2 = x_2^*$, $R_f = R_f^*$, for two different $x_{1,3}^{(1)}$ and $x_{1,3}^{(2)}$, we have $y_1^{(1)} = f_3^{(1)}(x_{1,3}^{(1)}, x_2^*, u^*) - R_f^* u^*$ and $y_1^{(2)} = f_3^{(2)}(x_{1,3}^{(2)}, x_2^*, u^*) - R_f^* u^*$. Using the property of monotonic increment, there are

$$\begin{aligned} sgn(y_1^{(1)} - y_1^{(2)}) &= sng(x_{1,3}^{(1)} - x_{1,3}^{(2)}) \\ &\Rightarrow sgn(f_3^{(1)}(x_{1,3}^{(1)}, x_2^*, u^*) - f_3^{(2)}(x_{1,3}^{(2)}, x_2^*, u^*)) \\ &= sgn(x_{1,3}^{(1)} - x_{1,3}^{(2)}) \end{aligned}$$

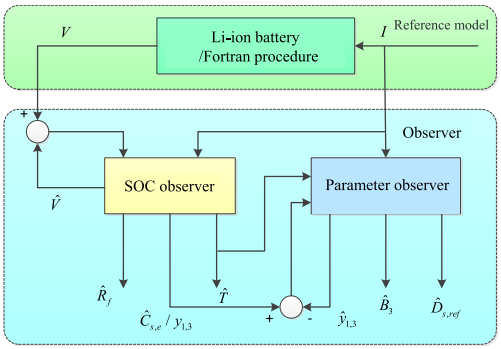

FIGURE 8. Architecture diagram of adaptive observer.

The SOC of the battery is related to the utilization rate of the cathode. It can be calculated by the concentration of lithium-ion on the solid surface, i.e. the state value of $x_{1,3}$. The formula is

$$SOC(t) = \frac{n_p(t) - n_{p0\%}}{n_{p100\%} - n_{p0\%}} \tag{60}$$

where $n_p(t) = \frac{x_{1,3}}{c_{s\max,p}}$.

The physical quantities that need to be estimated include SOC, temperature and the parameters that vary with temperature: solid diffusion coefficient D_s, electrochemical reaction rate constant k and contact resistance R_f. In addition, the output voltage and temperature are also required.

Therefore, the observers need to be built using the observed values y_1, y_2, u; the estimated state variables x_1, x_2; and the parameters θ, $R_{f,0}$, B_3. We design the observers as SOC observer and parameter observer, respectively. The structure of the observer is shown in Fig 8. The method of estimation separately can solve the state estimation effectively when the parameters change. The SOC observer obtains the current value u, the measured values y_1 and y_2 of terminal voltage and temperature from the physical or reference model of the battery, observes the surface concentration of solid spherical particles $\hat{x}_{1,3}$, temperature $\hat{x}_2$, and constant resistance parameter $R_{f,0}$, and transmits the observation results to the parameter observer. The parameter observer uses the results of SOC observer, i.e. the surface concentration of solid spherical particles is $\hat{x}_{1,3}$ and the temperature is $\hat{x}_2$, to observe the concentration distribution full state vector $\hat{x}_1$, the diffusion parameter θ and the B matrix parameter $\hat{B}_3$.

B. SOC OBSERVER DESIGN BASED ON ELECTROCHEMICAL-THERMAL COUPLING MODEL

In this paper, Lyapunov direct method is used to design the adaptive observer, and the stability of the adaptive observer is analyzed. When designing SOC observer, it mainly needs $x_{1,3}$ surface concentration to estimate SOC value, so a new state space equation is obtained by decomposing the whole model:

$$\begin{aligned}
\dot{R}_{f,0} &= 0 \\
\dot{x}_{1,3} &= \theta f_1(x_2)A_1x_{1,2} + \theta A_2 f_1(x_2)Ax_{1,3} + B_3u \\
\dot{x}_2 &= uf_2(x_{1,3}, x_2, y_1) - k(x_2 - x_{2,\infty}) \\
y_1 &= f_3(x_{1,3}, x_2, u) - R_{f,0}u - \alpha x_2 u \\
y_2 &= x_2
\end{aligned} \tag{61}$$

where $x_{1,3}$ is the surface concentration; $x_{1,2} \in R^2$ is a state vector of x_1 except $x_{1,3}$; $R_{f,0}$ is the position parameter; A_1 and A_2 are separated from the last dynamic characteristics of x_1. The system is an uncertain system, because θ, B_3 and $x_{1,2}$ have uncertainties.

The observer structure is constructed in the form of Lumberg observer:

$$\begin{aligned}
\dot{\widehat{x}}_{1,3} &= \bar{\theta} f_1(\widehat{x}_2)A_1\bar{x}_{1,2} + \bar{\theta}A_2 f_1(\widehat{x}_2)A\bar{x}_{1,3} + \bar{B}_3u + L_1(y_1 - \widehat{y}_1) \\
\dot{\widehat{x}}_2 &= uf_2(\widehat{x}_{1,3}, \widehat{x}_2, y_1) - k(\widehat{x}_2 - x_{2,\infty}) + L_2(y_2 - \widehat{y}_2) \\
\widehat{y}_1 &= f_3(\widehat{x}_{1,3}, \widehat{x}_2, u) - \widehat{R}_{f,0}u - \alpha\widehat{x}_2 u \\
\widehat{y}_2 &= \widehat{x}_2
\end{aligned} \tag{62}$$

Thus, the observer error dynamic characteristics can be described as:

$$\begin{aligned}
\dot{\widetilde{x}}_{1,3} &= F_1 - L_1\widetilde{y}_1 \\
\dot{\widetilde{x}}_2 &= u\widetilde{f}_2 - k\widetilde{x}_2 - L_2\widetilde{y}_2 \\
\widetilde{y}_1 &= \widetilde{f}_3 - \widetilde{R}_{f,0}u - \alpha\widetilde{x}_2 u \\
\widetilde{y}_2 &= \widetilde{x}_2
\end{aligned} \tag{63}$$

where $F_1 = \bar{\theta} f_1(\widehat{x}_2)A_1\bar{x}_{1,2} + \bar{\theta}A_2 f_1(\widehat{x}_2)A\bar{x}_{1,3} + \bar{B}_3u$, $\widetilde{f}_3 = f_3(x_{1,3}, x_2, u) - f_3(\widehat{x}_{1,3}, \widehat{x}_2, u)$, $\widetilde{f}_2 = f_2(x_{1,3}, x_2, u) - f_2(\widehat{x}_{1,3}, \widehat{x}_2, u)$, $\widehat{R}_{f,0} = R_{f,0} - \widehat{R}_{f,0}$, $\widetilde{x}_1 = x_1 - \widehat{x}_1$, $\widetilde{x}_2 = x_2 - \widehat{x}_2$, $\widetilde{y}_1 = y_1 - \widehat{y}_1$, $\widetilde{y}_2 = y_2 - \widehat{y}_2$, L_1 and L_2 are the observer gain to be determined.

Next, Lyapunov method is used to verify the stability of the observer, that is, the convergence of the error equation (63). Firstly, Lyapunov function is selected.

$$V = \frac{1}{2}\widetilde{x}_{1,3}^2 + \frac{1}{2}\widetilde{x}_2^2 + \frac{1}{2}\widetilde{R}_{f,0}^2 \tag{64}$$

Obviously, the function is positive definite. The derivation of equation (64) is obtained:

$$\begin{aligned}
\dot{V} &= \widetilde{x}_{1,3}\dot{\widetilde{x}}_{1,3} + \widetilde{x}_2\dot{\widetilde{x}}_2 + \widetilde{R}_{f,0}\dot{\widetilde{R}}_{f,0} \\
&\Rightarrow \dot{V} = \widetilde{x}_{1,3}(F_1 - L_1\widetilde{y}_1) + \widetilde{x}_2(u\widetilde{f}_2 - k\widetilde{x}_2 - L_2\widetilde{y}_2) - \widetilde{R}_{f,0}\dot{\widehat{R}}_{f,0} \\
&\Rightarrow \dot{V} = \widetilde{x}_{1,3}(F_1 - L_1\widetilde{f}_3) + \widetilde{x}_{1,3}L_1\widetilde{R}_{f,0}u + \widetilde{x}_2(u\widetilde{f}_2 \\
&\quad -k\widetilde{x}_2 - L_2\widetilde{y}_2 + \widetilde{x}_{1,3}L_1\alpha u) - \widetilde{R}_{f,0}\dot{\widehat{R}}_{f,0}
\end{aligned} \tag{65}$$

From the analysis of the above system characteristics, we can get $sgn(\widetilde{f}_3) = sgn(\widetilde{x}_{1,3})$, so there is $\widetilde{x}_{1,3}\widetilde{f}_3$, that is, $\widetilde{x}_{1,3}\widetilde{f}_3 = |\widetilde{x}_{1,3}||\widetilde{f}_3|$. And $\widetilde{y}_2 = \widetilde{x}_2$. Equation (65) can be rewritten as follows:

$$\begin{aligned}
\dot{V} &= (\widetilde{x}_{1,3}F_1 - L_1|\widetilde{x}_{1,3}||\widetilde{f}_3|) + (u\widetilde{f}_2\widetilde{x}_2 - (k \\
&\quad +L_2)\widetilde{x}_2^2 + \widetilde{x}_2\widetilde{x}_{1,3}L_1\alpha u) + \widetilde{x}_{1,3}L_1\widehat{R}_{f,0}u - \dot{\widehat{R}}_{f,0} \\
&\quad \xrightarrow[ab\le|ab|=|a||b|]{}
\end{aligned} \tag{66}$$

$$\begin{aligned}
\dot{V} &\le |\widetilde{x}_{1,3}|(|F_1| - L_1|\widetilde{f}_3|) + |\widetilde{x}_2|(|u\widetilde{f}_2| - (k + L_2)|\widetilde{x}_2| \\
&\quad +|\widetilde{x}_{1,3}L_1\alpha u|) + \widetilde{x}_{1,3}L_1\widehat{R}_{f,0}u - \widetilde{R}_{f,0}\dot{\widehat{R}}_{f,0}
\end{aligned} \tag{67}$$

The adaptive estimation rule of contact resistance R_f is:

$$\begin{aligned}
\dot{\widehat{R}}_{f,0} &= -L_3 sgn(u)sgn(\widetilde{y}_1) \\
\Rightarrow \dot{\widehat{R}}_{f,0} &= -L_3 sgn(u)sgn(\widetilde{f}_3 - \widetilde{R}_{f,0}u - \alpha\widetilde{x}_2 u)
\end{aligned} \tag{68}$$

Then,

$$\begin{aligned}\dot{V} \le\ & |\widetilde{x}_{1,3}|(|F_1| - L_1|\widetilde{f}_3|) + |\widetilde{x}_2|(|u\widetilde{f}_2| \\ & -(k+L_2)|\widetilde{x}_2| + |\widetilde{x}_{1,3}L_1\alpha u|) + \widetilde{x}_{1,3}L_1\widetilde{R}_{f,0}u \\ & +\widetilde{R}_{f,0}L_3 sgn(u)sgn(\widetilde{f}_3 - \widetilde{R}_{f,0}u - \alpha\widetilde{x}_2 u) \end{aligned} \tag{69}$$

As long as the Lyapunov function is positive definite and its derivative is semi-negative definite, the stability of the system can be obtained. For the first term of the right side of equation (69), if there is enough $L_1 > |F_1|/|\widetilde{f}_3|$, we can guarantee that $|\widetilde{x}_{1,3}|(|F_1| - L_1|\widetilde{f}_3|)$ is negative. For the second term on the right side of the equation, as long as there is $L_2 > (u\widetilde{f}_2|\widetilde{x}_{1,3}L_1\alpha u|)/|\widetilde{x}_2|$, $|\widetilde{x}_2|(|u\widetilde{f}_2| - (k+L_2)|\widetilde{x}_2| + |\widetilde{x}_{1,3}L_1\alpha u|)$ is guaranteed to be negative. For the third and fourth terms on the right side of the equation, using the system characteristics analyzed above, under the condition of $\widetilde{f}_3 < \widetilde{R}_{f,0}u$, we can get $sgn(\widetilde{h} - \widetilde{R}_{f,0}u - \alpha\widetilde{x}_2 u) = sgn(-\widetilde{R}_{f,0}u) = -sgn(\widetilde{R}_{f,0})sgn(u)$. Using $ab \le |ab| = |a||b|$, the equation (69) is transformed into:

$$\begin{aligned}\dot{V} \le\ & (\widetilde{x}_{1,3}F_1 - L_1|\widetilde{x}_{1,3}||\widetilde{f}_3|) + (u\widetilde{f}_2\widetilde{x}_2 - (k+L_2)\widetilde{x}_2^2 \\ & +\widetilde{x}_2\widetilde{x}_{1,3}L_1\alpha u) + |\widetilde{R}_{f,0}|(L_1|\widetilde{x}_{1,3}||u| - L_3) \end{aligned} \tag{70}$$

Similarly, we can get that L_3 should be a sufficiently large positive value that satisfies $L_1|\widetilde{x}_{1,3}||u| < L_3$ and $|\widetilde{f}_3| < |\widetilde{R}_{f,0}u|$.

Therefore, since $V > 0$, as long as observer gain L_1, L_2 and L_3 are large enough to satisfy $L_1 > |F_1|/|\widetilde{f}_3|$ and $|\widetilde{f}_3| < |\widetilde{R}_{f,0}u|$ respectively, $\dot{V} > 0$ can be achieved, and the SOC observer is stable.

Next, the parameter observer is designed. When designing the parameter observer, the unknown parameters θ and B_2 are adjusted mainly by $x_{1,3}$ and x_2. Similarly, the original system is decomposed and the output is changed to the lithium-ion concentration on the solid surface. There are:

$$\begin{aligned} \dot{\theta} &= 0 \\ \dot{B}_3 &= 0 \\ \dot{x_1} &= \theta f_1 x_2 A x_1 + [0, 0, B_3]^T u \\ y_{1,3} &= x_{1,3} = Cx_1, C = [0, 0, 1] \end{aligned} \tag{71}$$

where x_1 is the state variables of the transfer function of the relationship between lithium-ion concentration and current on the solid surface after Padé approximation, θ and B_3 are unknown parameters, and x_2 is the temperature estimated by the SOC observer. $y_{1,3} = x_{1,3}$ is the surface lithium-ion concentration estimated by SOC observer. The system assumes that parameters θ and B_3 change slowly, so there are $\dot{\theta}, \dot{B} = 0$. Because when L_1 and L_2 are large enough, the steady state values of $\widetilde{x}_{1,3}$ and $\widetilde{x}_2$ can be neglected in application. The observer is also constructed in the form of Lumberg observer:

$$\begin{aligned} \dot{\widehat{x}}_1 &= \widehat{\theta} f_1 x_2 A\widehat{x}_1 + [0, 0, \widehat{B}_3]^T u + L_4(y_{1,3} - \widehat{y}_{1,3}) \\ \widehat{y}_{1,3} &= C\widehat{x}_1 \end{aligned} \tag{72}$$

The dynamic characteristics of the observer error are as follows:

$$\begin{aligned} \dot{\widetilde{x}}_1 &= \theta f_1 x_2 A x_1 - \widehat{\theta} f_1 x_2 A\widehat{x}_1 + [0, 0, \widetilde{B}_3]^T u - L_4 y_{1,3} \\ \widetilde{y}_{1,3} &= C\widetilde{x}_1 \end{aligned} \tag{73}$$

Next, Lyapunov method is used to verify the stability of the observer, that is, the convergence of the error equation (73). First, Lyapunov function is selected:

$$V = \frac{1}{2}\widetilde{x}_1^T\widetilde{x}_1 + \frac{1}{2}K_1\widetilde{\theta}^2 + \frac{1}{2}K_2\widetilde{B}_3{}^2, \quad (K_1, K_2 > 0) \tag{74}$$

The derivative of Lyapunov function is obtained as follows:

$$\begin{aligned} \dot{V} &= \frac{1}{2}\dot{\widetilde{x}}_1^T\widetilde{x}_1 + \frac{1}{2}\dot{K_1}\widetilde{\theta}\dot{\widetilde{\theta}} + \frac{1}{2}\dot{K_2}\widetilde{B}_3\dot{\widetilde{B}}_3 \\ \Rightarrow \dot{V} &= \widetilde{x}_1^T(\theta f_1 A x_1 - \widehat{\theta} f_1 A\widehat{x}_1 - L_4\widetilde{y}_{1,3}) \\ &\quad +\widetilde{x}_1^T[0, 0, \widetilde{B}_3]^T u + \dot{K_1}\widetilde{\theta}\dot{\widetilde{\theta}}K_2\widetilde{B}_3\dot{\widetilde{B}}_3 \\ \Rightarrow \dot{V} &= (\theta f_1\widetilde{x}_1^T A x_1 - \widetilde{x}_1^T L_4 C\widetilde{x}_1) \\ &\quad +\widetilde{\theta}(f_1\widehat{x}_1^T A^T\widetilde{x}_1 - \dot{K_1}\dot{\widehat{\theta}}) + \widetilde{B}_3(\widetilde{y}_{1,3}u - \dot{K_2}\dot{\widehat{B}}_3) \end{aligned} \tag{75}$$

The adaptive estimation rules of θ and B_3 are:

$$\begin{aligned} \dot{\widehat{B}}_3 &= \widetilde{y}_{1,3}u/K_2 \\ \dot{\widehat{\theta}} &= f_1\widehat{x}_1^T A^T C^T\widetilde{y}_{1,3}/K_1 \end{aligned} \tag{76}$$

The equation (67) is rewritten as follows:

$$\dot{V} = \theta f_1\widetilde{x}_1^T A x_1 - \widetilde{x}_1^T L_4 C\widetilde{x}_1 \tag{77}$$

To make $\dot{V}$ semidefinite, the observer gain L_4 is selected to make L_4C semidefinite, i.e. $-\widetilde{x}_1^T L_4 C\widetilde{x}_1$. In addition, in the system A is semi-negative definite, function f_1 and parameter θ represent Arrhenius equation and solid diffusion coefficient. According to their physical characteristics, f_1 and θ are always positive. Hence, $\theta f_1\widetilde{x}_1^T A x_1 \le 0$. As a result, $\dot{V} \le 0$. Thus, it can be seen that the parameter observer is convergent, and both $\widetilde{\theta}$ and $\widetilde{B}_3$ are bounded. The Lyapunov analysis based on Barbalat lemma proves that the estimation error $\widetilde{\theta}$ and $\widetilde{B}_3$ converge to 0 gradually.

Barbalat lemma is a common lemma for stability analysis. In this paper, Barbalat lemma 2 is used. It is described as: Let $x : [0, \infty) \to R$ be continuous derivable of first order, and if $t \to \infty$, there is a limit, then $\lim_{n\to\infty} \dot{x}(t) = 0$ if $\ddot{x}(t)$, $t \in [0, \infty)$ exists and is bounded.

To prove the asymptotic convergence of $\widetilde{\theta}$ and $\widetilde{B}_3$, it is necessary to prove the asymptotic convergence of $\widetilde{x}_1$. Equation (67) can be transformed into

$$\dot{V} = -\widetilde{x}_1^T\beta\widetilde{x}_1 \le 0 \tag{78}$$

where, $\beta = \theta f_1 A - L_4 C$.

The derivative of $\dot{V}$ is obtained:

$$\ddot{V} = -2\dot{\widetilde{x}}_1^T\beta\dot{\widetilde{x}}_1 \tag{79}$$

where $\dot{\widetilde{x}}_1 = \theta f_1(x_2)Ax_1 - \widehat{\theta} f_1(x_2)A(\widehat{x}_1) + [0, 0, \widetilde{B}_3]^T u - L_4 C\dot{\widetilde{x}}_1$.

x_1, θ and B_3 are bounded by physical models. In addition, the input u is a current, there are limitations, also considered bounded. In previous Lyapunov analysis of parameter

observer, we know that estimation errors $\tilde{x}_1$, $\tilde{\theta}$ and $\tilde{B}_3$ are bounded. So estimates $\hat{x}_1$, $\hat{\theta}$ and $\hat{B}_3$ are also bounded. Thus, both $\dot{\tilde{x}}_1$ and $\dot{V}$ are bounded. Using Barbalat lemma, we can see that when $t \to \infty$, there is $\dot{V} \to \infty$. Because $\dot{V} = -\tilde{x}_1^T \beta \tilde{x}_1$, when $t \to \infty$, there is $\tilde{x}_1 \to 0$. So, the integral $\int_0^\infty \dot{\tilde{x}}_1 dt = \lim_{t\to\infty} \tilde{x}_1(t) - \tilde{x}_1(0) = -\tilde{x}_1(0)$, which tends to infinity, exists and is bounded. For the derivative of $\dot{\tilde{x}}_1$, we get:

$$\ddot{V} = \theta f_1(x_2) A \dot{x}_1 - \hat{\theta} f_1(x_2) A \dot{\hat{x}}_1 + [0, 0, \tilde{B}_3]^T \dot{u} - L_4 C \dot{\tilde{x}}_1 \quad (80)$$

Assuming that $\dot{u}$ is also bounded, given the conditions, $\ddot{\tilde{x}}_1$ is also bounded. Using Barbalat lemma, we can see that when $t \to \infty$, $\dot{\tilde{x}}_1 \to 0$. In addition, as shown in the previous section, when $t \to \infty$, $\tilde{x}_1 \to 0$. So there is:

$$\hat{\theta} f_1(x_2) A x_1 + [0, 0, \tilde{B}_3]^T u = 0 \quad (81)$$

Expand it and get

$$\left[[f_1(x_2) A x_1][0, \ldots, 0, u]^T \right] = \begin{bmatrix} \tilde{\theta} \\ \tilde{B}_3 \end{bmatrix} = 0 \quad (82)$$

Therefore, when $u \neq 0$, $\tilde{\theta}$ and $\tilde{B}_3$ are zero. That is, when $t \to \infty$, $\tilde{\theta}$ and $\tilde{B}_3$ tend to zero and have asymptotic convergence. Thus, the asymptotic convergence of $\tilde{\theta}$ and $\tilde{B}_3$ is proved.

IV. SIMULATION VERIFICATION OF SOC ESTIMATION FOR LIBs

In the III section, the construction method of adaptive observer is discussed. In order to verify the effectiveness and the stability of the proposed model, the simulation model is established and compared with the reference model under different operating conditions in this section. The charging and discharging experiments of LIBs with positive $LiCoO_2$ and negative MCMB2528 are carried. The cells have a rated capacity of 3400 mAh. The rated voltage is 3.7V, with the upper voltage being 4.2V. According to the content of the previous section, a simulation model is built in MATLAB/Simulink to simulate and test the built adaptive observer. In the simulation, the pseudo two-dimensional model considering the model changes in Fortran program is considered as a reference, so the reference equation (60) can process the data in Fortran program to get the reference SOC and use it as the true value.

New European Driving Conditions (NEDC) is used to verify the validity of battery model and SOC estimation with a duration of 1180s. The 0s to 1100s period of NEDC operating condition describes the driving condition at low speed, and the 1100s to 1180s period describes the driving condition at high speed. The driving condition is comprehensive. Converting the NEDC operating conditions into current is shown in Fig 9. The estimated results and errors of SOC are shown in Fig 10 and Fig 11. The main observation is whether the observed SOC can follow the true value of SOC well. In Fig 10, the blue curve is the SOC estimation of reference model, and the red curve is the observer SOC estimation

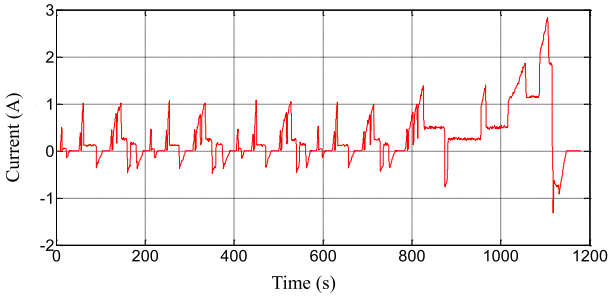

FIGURE 9. NEDC working current.

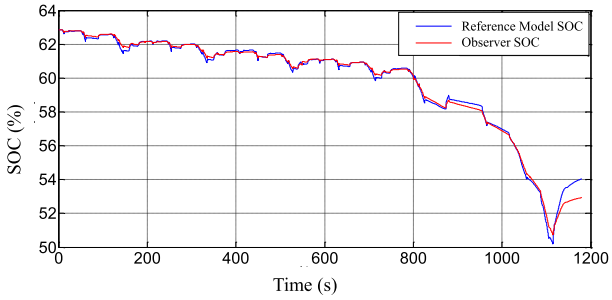

FIGURE 10. comparison of adaptive SOC observer estimation under NEDC operating condition.

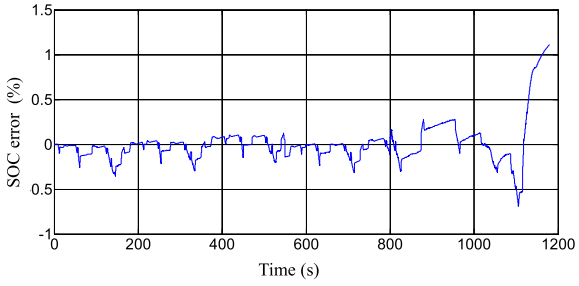

FIGURE 11. SOC estimation error under NEDC operating condition.

proposed in this paper. Before 1100s, SOC estimation error is less than 0.3%, which can be seen in Fig 11. After 1100s, the SOC estimation error increases obviously, and it is not sure whether it converges or not. The simulation results show that before 1100s, under the repeated action of the same small current condition, there is no obvious accumulation of errors, but a significant reduction due to the function of adaptive observer. After 1100s, the error increases obviously with the intense change of current, especially after the charge-discharge current becomes larger.

However, when the NEDC operating condition is presented, it is impossible to confirm whether the electrochemical-thermal coupling model applied to the observer in SOC estimation can still achieve better results in the case of more intense changes in current. Especially in the case of NEDC, the estimation error of SOC has a significant increase, but it can not judge whether the error diverges.

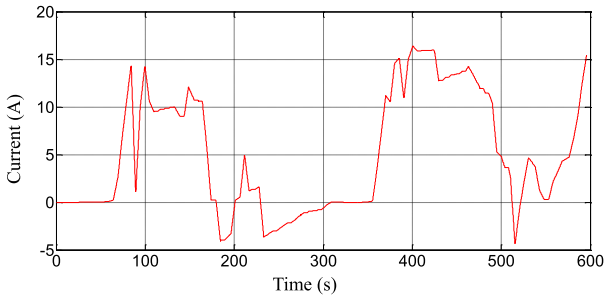

FIGURE 12. US06 working current.

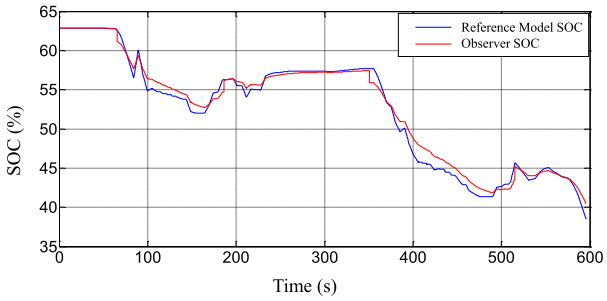

FIGURE 13. comparison of adaptive SOC observer estimation under US06 operating condition.

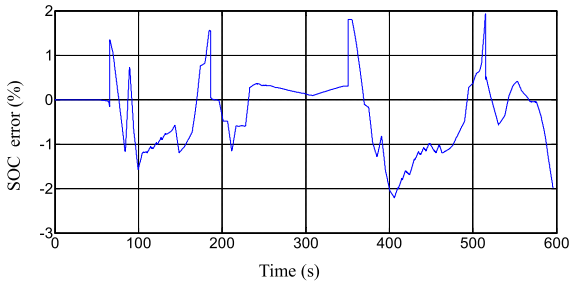

FIGURE 14. SOC estimation error under US06 operating condition.

Therefore, the US06 operating mode is selected for further verification. The US06 is one of the road conditions formulated by the United States. It simulates the driving conditions of highway with intense driving methods. It has high speed, high acceleration and frequent start and stop of vehicles, with the time of 596 seconds. The US06 operating mode is converted into current as shown in Fig 12. The results and errors of SOC estimation are shown in Fig 13 and Fig 14. It can be seen from the figure that US06 operating condition can be regarded as the extension of the large current of NEDC operating condition, because the charging and discharging current of US06 is relatively large and there is no repetitive working condition. As is shown in Fig 14, in this extreme case, the SOC estimation error of the observer increases obviously, but the error does not diverge at high current. And the maximum error is only about 2%. It also shows that the final error steep rise of NEDC is caused by the change of operating condition. And the error will not divergence if the latter works continuously with high current. It proves the effectiveness and stability of the observer.

V. CONCLUSION

In this paper, firstly, the working mechanism of LIBs is analyzed, and a pseudo two-dimensional model is derived. In order to solve two numerical problems of pseudo two-dimensional model, a one-dimensional model is proposed and simplified. Secondly, the principle of heat generation and heat exchange of LIBs are analyzed, and the electrochemical-thermal coupling model of LIBs is established. Then, the estimation problem based on coupling model is analyzed, and the coupling model is applied to SOC estimation. An adaptive SOC observer based on electrochemical-thermal coupling model is designed. Finally, Fortran program is used as battery to verify the designed adaptive observer.

ACKNOWLEDGMENT

The authors would like to thank the Editor-in-Chief, the Associate Editor, and the anonymous reviewers for their constructive comments, which helped improve the quality and presentation of this paper.

REFERENCES

[1] M. Yan, W. Liu, and G. Xiaojing, "Study on water cooling system with parallel loop of power battery pack based on AMESim," *J. Jilin Univ., Inf. Sci. Ed.*, vol. 35, no. 3, pp. 304–310, 2017.
[2] J. C. Maxwell, *A Treatise on Electricity and Magnetism*, vol. 2, 3rd ed. Oxford, U.K.: Clarendon, 1892, pp. 68–73.
[3] I. S. Jacobs and C. P. Bean, "Fine particles, thin films and exchange anisotropy," in *Magnetism*, vol. 3, G. T. Rado and H. Suhl, Eds. New York, NY, USA: Academic, 1963, pp. 271–350.
[4] M. A. Hannan, M. S. H. Lipu, A. Hussain, and A. Mohamed, "A review of lithium-ion battery state of charge estimation and management system in electric vehicle applications: Challenges and recommendations," *Renew. Sustain. Energy Rev.*, vol. 78, pp. 834–854, Oct. 2017.
[5] M. Doyle, T. F. Fuller, and J. Newman, "Modeling of galvanostatic charge and discharge of the lithium/polymer/insertion cell," *J. Electrochem. Soc.*, vol. 140, no. 6, pp. 1526–1533, 1993.
[6] P. Hui, "Multi-scale modeling and its simplification method of Li-ion battery based on electrochemical model," *Acta Phys. Sinica*, vol. 66, no. 23, pp. 306–316, 2017.
[7] Y. Ma, M. Yin, Z. Ying, and H. Chen, "Establishment and simulation of an electrode averaged model for a lithium-ion battery based on kinetic reactions," *RSC Adv.*, vol. 6, no. 30, pp. 25435–25443, 2016.
[8] Y. Ma, J. Ru, M. Yin, H. Chen, and W. Zheng, "Electrochemical modeling and parameter identification based on bacterial foraging optimization algorithm for lithium-ion batteries," *J. Appl. Electrochem.*, vol. 46, no. 11, pp. 1119–1131, 2016.
[9] S. Tang, L. Camachosolorio, Y. Wang, and M. Krsti, "State-of-charge estimation from a thermal–electrochemical model of lithium-ion batteries," *Automatica*, vol. 83, pp. 206–219, Sep. 2017.
[10] Q. Wang, J. Wang, P. Zhao, J. Kang, F. Yan, and C. Du, "Correlation between the model accuracy and model-based SOC estimation," *Electrochim. Acta*, vol. 228, pp. 146–159, Feb. 2017.
[11] X. Lin, "On the analytic accuracy of battery SOC, capacity and resistance estimation," in *Proc. Amer. Control Conf.*, Jul. 2016, pp. 4006–4011.
[12] J. C. Forman, S. Bashash, J. L. Stein, and H. K. Fathy, "Reduction of an electrochemistry-based li-ion battery model via quasi-linearization and pade approximation," *Electrochem. Soc.*, vol. 158, no. 2, pp. A93–A101, 2011.
[13] T. Jacobsen and K. West, "Diffusion impedance in planar, cylindrical and spherical symmetry," *Electrochim. Acta*, vol. 40, no. 2, pp. 255–262, 1995.
[14] B. Li, "Research on modeling and SOC estimation of temperature-dependent electric vehicle power battery," Jilin Univ., Jilin, China, Tech. Rep., 2017.

YAN MA received the B.S. degree in automation from the Department of Automation, Harbin Engineering University, Harbin, China, in 1992, and the M.S. degree in control theory and control engineering and the Ph.D. degree in communication and information system from the Department of Control Science and Engineering, Jilin University, Changchun, China, in 1995 and 2006, respectively. In 1995, she joined the former Jilin University of Technology. She held a postdoctoral positon at Poly U, Hong Kong. Since 2009, she has been a Professor with Jilin University. Her current research interests include nonlinear estimation methods, applications in power management systems of electric vehicles and robust filter methods, such as state of charge (SOC) estimation, state of health estimation, state of power estimation, and battery equalization.

XIN LI was born in Hebei, China. She received the B.S. degree in automation from the Aviation Automation College, Civil Aviation University of China, Tianjin, China, and the M.S. degrees in control theory and control engineering from Northeast Dianli University, Jilin, China, in 2015 and 2018, respectively. She is currently pursuing the Ph.D. degree in control theory and control engineering with the Department of Control Science and Engineering, Jilin University, Changchun, China. Her research interests include battery management systems and battery temperature control systems of electric vehicles, which include state of charge estimation, state of health estimation, state of power estimation, and battery equalization.

GUANGYUAN LI was born in Henan, China. He received the B.S. degree in automation and the M.S. degree in control theory and control engineering from Jilin University, Changchun, China, in 2015 and 2018, respectively. He is currently pursuing the Ph.D. degree with the School of Transportation Science and Engineering, Beihang University, Beijing, China.

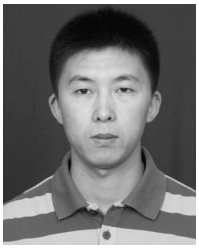

YUNFENG HU received the M.S. degree in basic mathematics and the Ph.D. degree in control theory and control engineering from Jilin University, Changchun, China, in 2008 and 2012, respectively. He is currently an Associate Professor with the Department of Control Science and Engineering, Jilin University. His current research interests include nonlinear control and automotive control.

QINGWEN BAI was born in Jilin, China. He received the B.S. degree in automation and the M.S. degree in control science and engineering from Jilin University, China, in 2010 and 2013, respectively. He is currently a Product-Engineer with the Department of Electrics & Electronics Engineering, FAW-Volkswagen Company Ltd, Changchun. His research interests include battery management systems and battery temperature control systems of electric vehicles, which include state of charge estimation, state of health estimation, state of power estimation, and battery equalization.